MECHANISM OF DISSIMILAR MOMENTUM AND HEAT TRANSFER INDUCED BY A TRAVELING WAVE-LIKE BLOWING/SUCTION IN TURBULENT CHANNEL FLOW

Yosuke Hasegawa[1,2], **Nobuhide Kasagi**[1]
[1]Department of Mechanical Engineering
The University of Tokyo
Hongo 7-3-1 Bunkyo-ku, Tokyo, Japan
hasegawa/kasagi@thtlab.t.u-tokyo.ac.jp

[2]Center of Smart Interfaces
Technical University Darmstadt
Petersenstr. 32, 64287 Darmstadt, Germany
hasegawa@csi.tu-darmstadt.de

ABSTRACT

The suboptimal control theory is applied for achieving dissimilar control of enhancing heat transfer, while keeping the skin friction not increased considerably in a fully developed channel flow. The Fréchet differentials clearly show that the responses of velocity and temperature fields to wall blowing/suction are quite different due to the fact that the velocity is a divergence-free vector while the temperature is a conservative scalar. This essential difference allows us to achieve dissimilar control even in flows where the averaged momentum and energy transport equations have the identical form. It is also found that the resultant optimized mode of control input exhibits a streamwise traveling wave-like property. By exploring the phase relationship between the traveling wave-like control input and the velocity and thermal fields, we reveal that such control input contributes to dissimilar heat transfer enhancement via two different mechanisms.

INTRODUCTION

Enhancement of heat and mass transfer in various thermal-fluids systems should be of growing importance not only for energy saving, but also for economy and the environment. When doing this, the wall skin friction, against which fluid is driven by pumping power, should be reduced, since the work done is eventually dissipated by the fluid viscosity. This dissimilar enhancement/reduction control, however, is difficult to achieve owing to the similarity between the momentum and energy transport processes. Recently, Kasagi et al. (2011) reexamined the transport equations and the wall boundary conditions for the velocity and thermal fields, and summarized possible strategies for achieving dissimilar control. Among these strategies, dissimilar control based on the inherent difference between divergence-free vector and conservative scalar has also been demonstrated. By exploiting this inherent difference, Hasegawa and Kasagi (2010) showed that significant dissimilar control is actually possible even under an ideal condition, where the averaged momentum and heat transport equations have the identical form. They have also found that the control input derived from the suboptimal control theory exhibits a traveling wave-like property. In the present study, we extend the previous work in order to clarify the features of this unique control and the mechanism of dissimilarity. We aim to eventually obtain general knowledge for dissimilar control for practical applications.

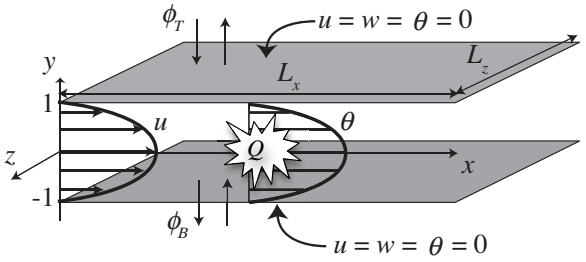

Figure 1. Computational domain and coordinate system.

MATHEMATICAL FORMULATION

Numerical Scheme and Test Condition

We consider a fully developed turbulent channel flow under a constant mass flow rate. The coordinate system and thermal conditions are shown in Fig. 1. The fluid properties are assumed constant and the temperature is a passive scalar without any buoyancy effect. The governing equations for the flow and thermal fields are the following Navier-Stokes, continuity

and energy transport equations:

$$\frac{\partial u_i}{\partial t}+\frac{\partial (u_j u_i)}{\partial x_j}=-\frac{\partial p}{\partial x_i}+\frac{1}{\mathrm{Re}}\frac{\partial u_i^2}{\partial x_j \partial x_j}, \tag{1}$$

$$\frac{\partial u_i}{\partial x_i}=0, \tag{2}$$

$$\frac{\partial \theta}{\partial t}+\frac{\partial (u_j \theta)}{\partial x_j}=Q+\frac{1}{\mathrm{PrRe}}\frac{\partial \theta^2}{\partial x_j \partial x_j}. \tag{3}$$

Throughout this paper, all quantities are normalized by the bulk velocity U_b^*, the channel half depth δ^* and the bulk temperature Θ_b^* defined below. The asterisk denotes a dimensional quantity. The Reynolds number is set to be $\mathrm{Re}=U_b^*\delta^*/\nu^*=2280$, which corresponds to the friction Reynolds number of $\mathrm{Re}_\tau=u_\tau^*\delta^*/\nu^*=150$ in uncontrolled flow, where u_τ^* and ν^* are the friction velocity and the fluid kinematic viscosity, respectively. Uniform heat generation Q is assumed to be equal to the mean pressure gradient. In addition, the Prandtl number Pr is unity throughout this study, so that the resultant averaged transport equations for the streamwise velocity $\overline{u}$ and the temperature $\overline{\theta}$ have the identical form as:

$$-\frac{\partial \overline{p}}{\partial x}=\frac{d}{dy}\left(\overline{u'v'}-\frac{1}{\mathrm{Re}}\frac{d\overline{u}}{dy}\right), \tag{4}$$

$$Q=-\frac{\partial \overline{p}}{\partial x}=\frac{d}{dy}\left(\overline{\theta'v'}-\frac{1}{\mathrm{Re}}\frac{d\overline{\theta}}{dy}\right), \tag{5}$$

where the over-bar represents averaging in the homogeneous directions, i.e., the x and z directions and also time t. In the present study, we consider local wall blowing/suction with no net mass flux as a control input. As for the tangential velocity components and the temperature, we impose the no-slip and constant-temperature conditions at the top and bottom walls, i.e., $y=-1$ and 1, respectively. The resultant Dirichlet-type boundary conditions are given as:

$$u_i=\phi_B\delta_{i2},\ \theta=0 \quad \text{at } y=-1, \tag{6}$$

$$u_i=\phi_T\delta_{i2},\ \theta=0 \quad \text{at } y=1, \tag{7}$$

where ϕ_B and ϕ_T are control inputs (given velocity) at the bottom and top walls, respectively. Note that the wall boundary conditions for the streamwise velocity component and the temperature remain similar even in the controlled flow, i.e., $u=\theta=0$ at the walls.

Equations (1)-(3) are solved by a pseudo-spectral method, where Fourier expansion is employed in the x and z directions, while Chebyshev polynomials in the y direction. The number of modes employed in each direction is $(k_1,k_2,k_3)=(64,65,64)$. Details of numerical scheme and its verification can be found in Hasegawa and Kasagi (2011).

Control Performance Indices

The bulk mean velocity U_b^* is generally defined based on the total mass flow rate as:

$$U_b^*=\frac{1}{2\delta^*}\int_{-\delta^*}^{\delta^*}\overline{u^*}dy. \tag{8}$$

Similarly, the bulk temperature Θ_b^* in the present study is defined as:

$$\Theta_b^*=\frac{1}{2\delta^*}\int_{-\delta^*}^{\delta^*}\overline{\theta}^* dy. \tag{9}$$

Conventionally, the bulk temperature, which is often referred to as the mixing-cup temperature, has been defined based on the streamwise-velocity-weighted temperature so that it can be related to the streamwise enthalpy flux. However, this definition leads to a quantitative difference between the friction coefficient C_f and the Stanton number St defined below even though the velocity and temperature profiles are similar. The similar form of Eq. (9) to that of Eq.(8) assures $2\mathrm{St}/C_f=1.0$ as long as the profiles of $\overline{u}$ and $\overline{\theta}$ are similar. We also note that the present definition of Θ_b^* is generally underestimated than the conventional one by about 6%. However, this hardly influences the present results, since the increase rate of St, which is a major concern in the present study, is not significantly changed due to the present definition.

The definitions of C_f and St are given by:

$$C_f=\frac{\tau_w^*}{\frac{1}{2}\rho U_b^{*2}}, \tag{10}$$

$$\mathrm{St}=\frac{q_w^*}{\rho^* C_p^* U_b^* \Theta_b^*}, \tag{11}$$

where τ_w^* and q_w^* are the wall friction and the wall heat flux, while ρ^* and C_p^* are the fluid density and the thermal capacity of fluid, respectively.

Recently, Fukagata et al. (2002) have derived mathematical relationship between C_f and different dynamical contributions in wall-bounded flows. It is simplified to the following equation in a fully developed turbulent channel flows:

$$C_f=\frac{6}{\mathrm{Re}}+3\int_{-1}^{1}y(\overline{u'v'})\,dy. \tag{12}$$

The first term on the RHS of Eq. (12) corresponds to the laminar drag, while the second the additional friction due to turbulence. The Reynolds shear stress $\overline{u'v'}$, which is weighted by y in the second term on the RHS of Eq. (12), implies that the Reynolds shear stress near the wall contributes more to the skin friction drag than that in the central region of the channel. Similarly, we can also derive the following relationship for St:

$$2\mathrm{St}=\frac{6}{\mathrm{Re}}+3\int_{-1}^{1}y(\overline{\theta'v'})\,dy, \tag{13}$$

which has the same form as that of C_f in Eq. (12), indicating that dissimilarity between $\overline{u'v'}$ and $\overline{\theta'v'}$ is mandatory to achieve dissimilar control. The analogy factor A is defined as:

$$A=\frac{2\mathrm{St}_m}{C_f}. \tag{14}$$

Then, the main objective of this study is to demonstrate a possibility to increase A from unity by modifying turbulence.

APPLICATION OF SUBOPTIMAL CONTROL

Derivation of Differential States

Following Lee et al. (1998), we discretize the Navier-Stokes and energy equations so that the diffusion and pressure gradient terms are treated implicitly, while the advection terms explicitly. This results in the following equations representing the short-time dynamics of the system:

$$u_i^{n+1} + \frac{\Delta t}{2}\frac{\partial p^{n+1}}{\partial x} - \frac{\Delta t}{2\mathrm{Re}}\frac{\partial^2 u_i^{n+1}}{\partial x_j \partial x_j} = R^n, \tag{15}$$

$$\frac{\partial u_i^{n+1}}{\partial x_i} = 0, \tag{16}$$

$$\theta^{n+1} - \frac{\Delta t}{2\mathrm{Re}}\frac{\partial^2 \theta^{n+1}}{\partial x_j \partial x_j} = Q^n, \tag{17}$$

where R^n and Q^n represent the advection terms, while the superscript a time step. The Fréchet differentials q_i and η of the velocity and thermal fields with respect to the perturbation $\tilde{\phi}$ of control input can be derived as:

$$\begin{aligned}\widehat{q_1}(y) = \frac{ik_1}{k\cdot\sinh(2k)}\Bigg[&\widehat{\tilde{\phi}}_T\cosh\{k(y+1)\} - \widehat{\tilde{\phi}}_B\cosh\{k(y-1)\} \\ &-\left\{\widehat{\tilde{\phi}}_T\cosh(2k) - \widehat{\tilde{\phi}}_B\right\}\exp\left\{-\sqrt{\frac{2\mathrm{Re}}{\Delta t}}(1-y)\right\} \\ &-\left\{\widehat{\tilde{\phi}}_T - \widehat{\tilde{\phi}}_B\cosh(2k)\right\}\exp\left\{-\sqrt{\frac{2\mathrm{Re}}{\Delta t}}(y+1)\right\}\Bigg],\end{aligned} \tag{18}$$

$$\widehat{q_2}(y) = \frac{1}{\sinh(2k)}\left[\widehat{\tilde{\phi}}_T\sinh\{k(y+1)\} - \widehat{\tilde{\phi}}_B\sinh\{k(y-1)\}\right], \tag{19}$$

$$\hat{\eta}(y) = 0. \tag{20}$$

Here, a variable with a hat represents a Fourier coefficient and $k = \sqrt{k_1^2 + k_3^2}$, where k_1 and k_3 are wavenumbers in the x and z directions, respectively. When wall blowing/suction is applied, the pressure field instantaneously reacts to it and redistributes the kinetic energy of the wall-normal velocity fluctuation to the tangential components. This is caused by the continuity constraint on the velocity field. In the case of the scalar field, however, there exists no pressure-gradient term in Eqs. (17), and therefore η vanishes (see, Eq. (20)). This fact shows an essential difference between the responses of the velocity and scalar fields to the control input and suggests a possibility of dissimilar control.

Defining Cost Function

We define the cost function J as follows:

$$\begin{aligned}J = &\frac{1}{S\Delta t}\int_S\int_t^{t+\Delta t}\frac{1}{2}(\phi_T^2 + \phi_B^2)dtdS \\ &+ \frac{1}{V\Delta t}\int_V\int_t^{t+\Delta t}\beta\,(yu_1'u_2') - \gamma(y\theta' u_2')\,dtdV,\end{aligned} \tag{21}$$

where the temporal integration is made over a short duration of computational time step Δt. The spatial integration is also made over the wall surface (S) for the first term, whilst over the whole flow domain (V) for the second and third terms. Our goal is to deduce the optimal spatio-temporal distribution of control input ϕ to minimize J.

The first term on the RHS of Eq. (21) represents the cost of actuation. In accordance with Eqs. (12) and (13), we add the weighted Reynolds stress and weighted turbulent heat flux, which appear in the second integral, in order to evaluate friction drag and heat transfer, respectively. The coefficients of β and γ correspond to the relative costs of friction drag and heat transfer to the control input, respectively. We give a negative sign to γ so as to seek the least control input that maximizes the heat transfer while reducing the friction drag.

Derivation of Control Input

By applying a Fréchet differential to the cost function (21) and substituting Eqs. (18)−(20), minimizing J requires the following control inputs at bottom and top walls:

$$\begin{aligned}\hat{\phi}_B = \beta\int_{-1}^{1} y\left\{\frac{\sinh\{k(y-1)\}}{\sinh(2k)}\hat{u}_1(y) - \frac{ik_1\cosh\{k(y-1)\}}{k\cdot\sinh(2k)}\hat{u}_2(y)\right\}dy \\ - \gamma\int_{-1}^{1} y\left\{\frac{\sinh\{k(y-1)\}}{\sinh(2k)}\hat{\theta}(y)\right\}dy,\end{aligned} \tag{22}$$

$$\begin{aligned}\hat{\phi}_T = \beta\int_{-1}^{1} y\left\{\frac{ik_1\cosh\{k(y+1)\}}{k\cdot\sinh(2k)}\hat{u}_2(y) - \frac{\sinh\{k(y+1)\}}{\sinh(2k)}\hat{u}_1(y)\right\}dy \\ + \gamma\int_{-1}^{1} y\left\{\frac{\sinh\{k(y+1)\}}{\sinh(2k)}\hat{\theta}(y)\right\}dy.\end{aligned} \tag{23}$$

Detailed derivations of the Fréchet differentials (18)−(20) and the control inputs can be found in Hasegawa and Kasagi (2011).

CONTROL PERFORMANCE

In the present study, the magnitudes of the control inputs relative to the bulk mean velocity U_b at the two walls are kept constant as $\phi_{rms}/U_b = 0.05$ by rescaling Eqs. (22) and (23) at every time step, so that only the ratio of β and γ is of concern. The friction factor and the Stanton number normalized by those in the uncontrolled flow, and also the resultant analogy factor are plotted as a function of β/γ in Fig. 2. With decreasing β/γ, C_f and St commonly increase. However, St increases more rapidly than C_f. As a result, A is enhanced from unity significantly. In the present study, we focus on the case at $\beta/\gamma = 1.0$ since the largest A is achieved. In this case, St is increased by roughly three times from the uncontrolled value, while C_f remains doubled, so that $A = 1.5$ is obtained.

The averaged streamwise velocity $\overline{u}$ and temperature $\overline{\theta}$ profiles are shown in Fig. 3. In uncontrolled flow, $\overline{u}$ and $\overline{\theta}$ agrees quite well, so that A remains almost unity. When the dissimilar control is applied, both gradients of the mean velocity and temperature at the wall are larger than those in the uncontrolled flow. This results in the increase of friction drag and heat transfer. With the distance from the wall, both the mean velocity and temperature once become smaller than

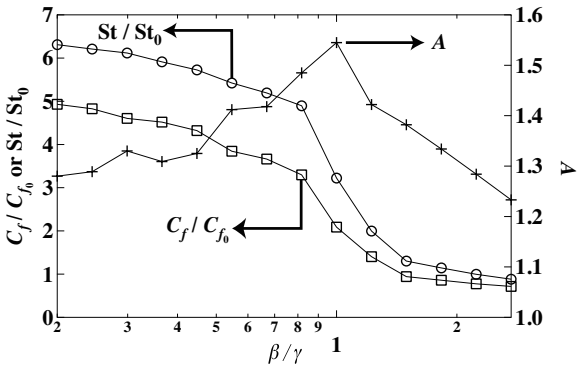

Figure 2. C_f and St normalized by the values in uncontrolled flow, and analogy factor $A = 2\mathrm{St}/C_f$ at different β/γ.

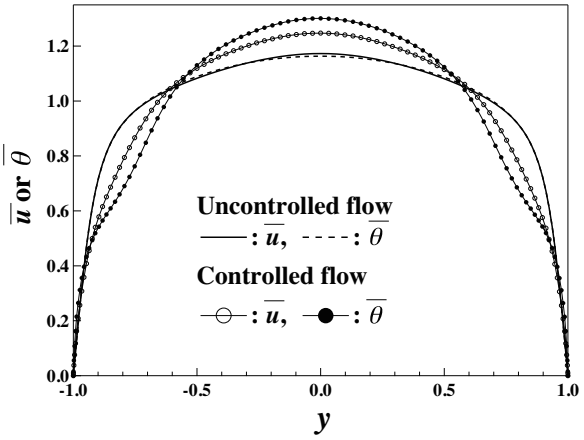

Figure 3. Averaged streamwise velocity $\overline{u}$ and temperature $\overline{\theta}$ in uncontrolled and controlled flows

those in the uncontrolled flow at $0.1\delta - 0.5\delta$, and then much larger in the central region. This modification is more pronounced in the temperature profile. As will be discussed later, they are attributed to the traveling wave-like control input.

DISSIMILAR MECHANISMS

Properties of Control Input

Kasagi et al. (2011) and Hasegawa and Kasagi (2010) show that the optimized control input in the present control exhibits a streamwise traveling wave-like property, which is almost uniform in the z direction. In order to examine the phase relationship between the traveling wave-like control input and the velocity and thermal fields, we extract the coherent part of the control input by applying a conditional averaging technique. First, the instantaneous control input at the bottom wall is averaged in the spanwise direction and the location x_p where the spanwise-averaged wall blowing becomes maximum is identified. Then, the control input at each wall is averaged with respect to x_p over a sufficiently long period after the velocity and thermal fields reach the fully developed state. As a result, the instantaneous control inputs ϕ at the two

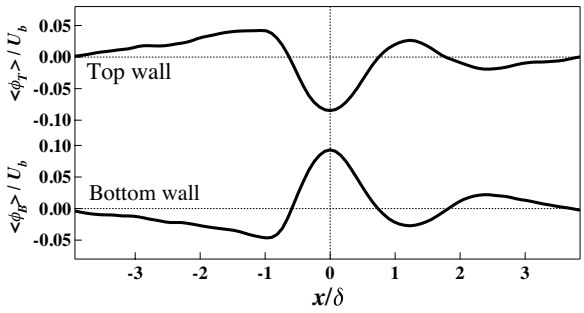

Figure 4. Distributions of conditionally averaged control inputs $\langle\phi\rangle$ at top and bottom walls

walls can be described as:

$$\phi(x,z,t) = \langle\phi\rangle(x - x_p(t)) + \phi''(x - x_p(t), z, t), \qquad (24)$$

where the angle bracket represents the conditional averaging, while the double prime the deviation from it.

The conditionally-averaged control inputs $\langle\phi_B\rangle$ and $\langle\phi_T\rangle$ at the bottom and top walls are shown in Fig. 4. Surprisingly, $\langle\phi_B\rangle$ and $\langle\phi_T\rangle$ are almost symmetric, indicating that the control is in a varicose-mode. The control input is characterized by strong blowing from a narrow spanwise band and weaker suction upstream of the blowing region. This coherent component accounts for 65% of the root-mean-square value of the instantaneous control input. In addition, x_p travels downstream at an almost constant phase speed of $0.3U_b$ (not shown here). Since statistical quantities in controlled flow are generally symmetric, we hereafter will show results only in the lower half of the computational domain, i.e., $-1 < y < 0$.

Dynamical Contributions to Dissimilarity

In accordance with the decomposition of the control input ϕ defined by Eq. (24), the instantaneous velocity and temperature in the controlled flow can also be expressed as:

$$\begin{aligned} c(x,y,z,t) &= \langle c\rangle(x - x_p, y) + c''(x - x_p, y, z, t) \\ &= \overline{c}(y) + \tilde{c}(x - x_p, y) + c''(x - x_p, y, z, t), \end{aligned} \qquad (25)$$

where c denotes an arbitrary quantity such as velocity components, pressure and temperature. A conditionally-averaged quantity with angle brackets is further decomposed into mean and coherent components represented by an over-bar and a tilde, respectively.

By applying the decomposition defined by Eq. (25) to Eqs. (12) and (13), dissimilarity between 2St and C_f can be expressed as:

$$2\mathrm{St} - C_f = 3\int_{-1}^{1} y\left\{\left(\overline{\tilde{\theta}\tilde{v}} - \overline{\tilde{u}\tilde{v}}\right) + \left(\overline{\theta'' v''} - \overline{u'' v''}\right)\right\} dy. \qquad (26)$$

This indicates that the dissimilarity is attributed to coherent and random contributions appearing as the fist and second

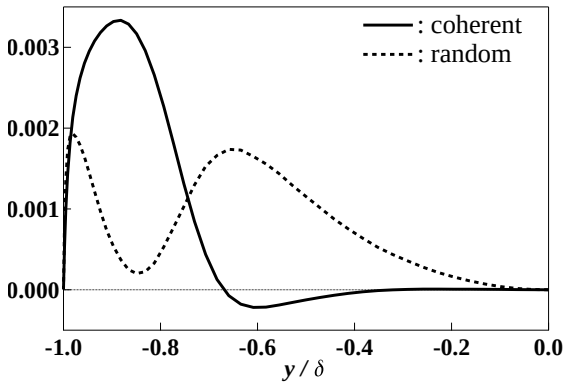

Figure 5. Differences between weighted turbulent heat flux and Reynolds shear stress, $y(\overline{\tilde{\theta}\tilde{v}} - \overline{\tilde{u}\tilde{v}})$ and $y(\overline{\theta''v''} - \overline{u''v''})$ in coherent and random components.

terms on the right-hand-side. The profiles of the two integrands, i.e., $y(\overline{\tilde{\theta}\tilde{v}} - \overline{\tilde{u}\tilde{v}})$ and $y(\overline{\theta''v''} - \overline{u''v''})$ are shown in Fig. 5. It is found that $y(\overline{\tilde{\theta}\tilde{v}} - \overline{\tilde{u}\tilde{v}})$ has a strong peak near the wall, while $y(\overline{\theta''v''} - \overline{u''v''})$ has two peaks in the vicinity of the wall, $y \approx -0.95$, and also far away from the wall, $y \approx -0.6$. Hereafter, we refer to the two contributions from $y(\overline{\tilde{\theta}\tilde{v}} - \overline{\tilde{u}\tilde{v}})$ and $y(\overline{\theta''v''} - \overline{u''v''})$ as direct and indirect effects, respectively.

Direct Effect

The conditionally-averaged wall-normal velocity $\tilde{v}$ and pressure $\langle p \rangle$ are plotted in Figs. 6 a) and b). Note that the mean pressure gradient is subtracted from $\langle p \rangle$. The wall-normal velocity $\tilde{v}$ reaches its maximum around 0.25δ away from the wall above the wall blowing. The wall blowing generates significant positive and negative pressure fluctuations in its upstream and downstream regions, respectively.

The induced pressure fluctuation causes significant dissimilarity between $\tilde{u}$ and $\tilde{\theta}$ as shown in Fig. 6 c). Upstream of the abrupt wall blowing, $\tilde{u}$ is generally smaller than $\tilde{\theta}$, i.e., $\tilde{\theta} - \tilde{u} < 0$, due to adverse pressure gradient induced by the wall blowing. In contrast, above the wall blowing region, strong favorable pressure gradient causes $\tilde{\theta} - \tilde{u} > 0$ in the downstream region. Consequently, a region with large positive $y(\tilde{\theta}\tilde{v} - \tilde{u}\tilde{v})$ is confirmed just above the abrupt wall blowing in Fig. 6 d). This is a primary reason for the prominent peak of $y(\overline{\tilde{\theta}\tilde{v}} - \overline{\tilde{u}\tilde{v}})$ near the wall observed in Fig. 5.

Indirect Effect

Since the mean velocity and temperature profiles in the controlled flow are no longer similar (see, Fig. 3), the dissimilarity between $\overline{u''v''}$ and $\overline{\theta''v''}$ should be discussed through comparison between the eddy diffusivities for momentum E_v'' and heat E_c'', rather than $\overline{u''v''}$ and $\overline{\theta''v''}$ themselves. We define these quantities in the controlled flow as follows:

$$E_v'' = \frac{-\overline{u''v''}}{\left(\dfrac{d\overline{u}}{dy}\right)}, \quad E_c'' = \frac{-\overline{\theta''v''}}{\left(\dfrac{d\overline{\theta}}{dy}\right)}. \tag{27}$$

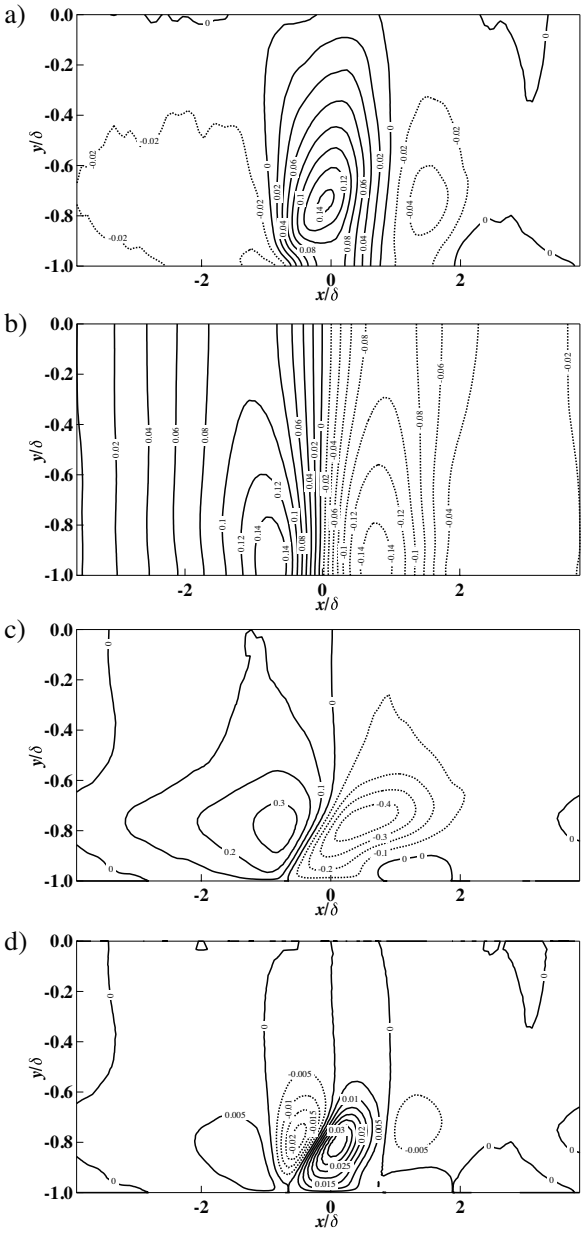

Figure 6. Distributions of coherent components a) wall-normal velocity component $\tilde{v}$, b) pressure $\langle p \rangle$, c) difference between temperature and streamwise velocity component $\tilde{\theta} - \tilde{u}$, d) difference in weighted turbulent heat flux and Reynolds stress $y(\tilde{\theta}\tilde{v} - \tilde{u}\tilde{v})$.

Then, $\overline{\theta''v''} - \overline{u''v''}$ is expressed as:

$$\overline{\theta''v''} - \overline{u''v''} = (\mathrm{Pr}_t''^{-1} S - 1)\overline{u''v''}. \tag{28}$$

Here, $S = (d\overline{\theta}/dy)/(d\overline{u}/dy)$ is the ratio of the mean temperature and velocity gradients. The turbulent Prandtl number is defined as $\mathrm{Pr}_t'' = E_v''/E_c''$. The above equation indicates that the dissimilarity between $\overline{\theta''v''}$ and $\overline{u''v''}$ is caused by enhancement of either $\mathrm{Pr}_t''^{-1}$ or S.

Distributions of $\mathrm{Pr}_t''^{-1}$ and S are plotted in Figs. 7 and 8,

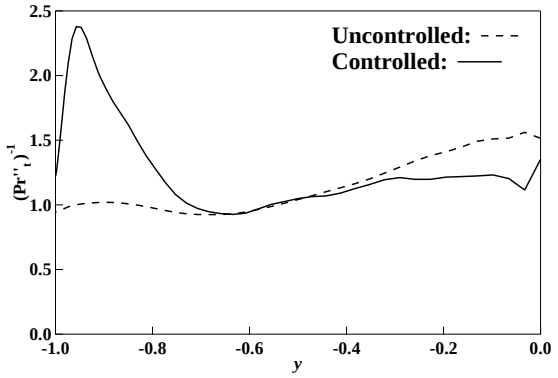

Figure 7. Turbulent Prandtl number in uncontrolled and controlled flows.

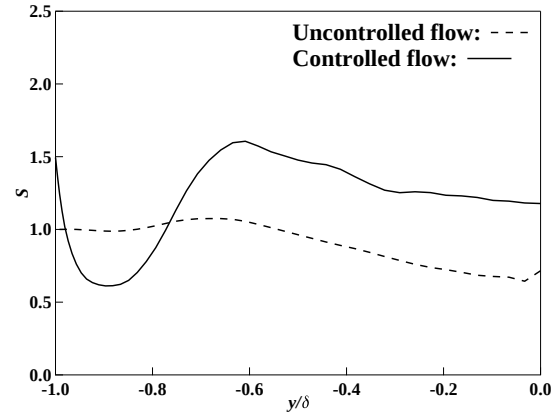

Figure 8. Ratio S of the mean temperature and velocity gradients in uncontrolled and controlled flows.

respectively. The data in uncontrolled flow are also shown for comparison. It is found that Pr''^{-1}_t increases in the near-wall region, while it is almost unchanged or even slightly decreased far from the wall at $y > -0.6$. In contrast, S exceeds unity in the very vicinity of the wall, whereas it first decreases rapidly with increasing the distance from the wall, and then becomes larger than the value of the uncontrolled flow again further away from the wall. Note that the limiting value of S at the wall should be identical to A. From Figs. 7 and 8, we conclude that the two peaks of $y(\overline{\theta''v''} - \overline{u''v''})$ observed in Fig. 5 are caused by different mechanisms, namely, the first peak near the wall is attributed to the increase in Pr''^{-1}_t, whereas the second peak away from the wall to the increase in S.

Recently, Hasegawa and Kasagi (2011) conduct additional computation, where only the coherent component of the control input is applied. In this calculation, the increase of S away from the wall is still observed, whereas the peak of Pr''^{-1}_t near the wall disappears. These results suggest that the former is caused by the coherent traveling wave-like input $\langle\phi\rangle$, whereas the latter is attributed to the random component ϕ'' of the control input.

CONCLUSIONS

Focusing on the inherent difference between the divergence-free vector and conservative scalar quantities, we demonstrate dissimilar control of momentum and heat transfer in a fully developed channel flow under the most difficult case, where the averaged transport equations and the wall boundary conditions for the streamwise velocity component and the temperature are identical.

The obtained control input exhibits a traveling wave-like property characterized by localized wall blowing from a narrow spanwise band associated with weak suction more evenly distributed in the upstream of the blowing. This wave travels in the downstream direction at an almost constant speed, i.e., about 30% of the bulk mean velocity. In addition, the control inputs at two opposing walls are applied in a varicose-mode.

The traveling wave-like control input contributes to dissimilar heat transfer enhancement through two distinct mechanisms, i.e., direct and indirect effects. The former is caused by the direct modification of the coherent velocity and thermal fields, which results in dissimilarity between the coherent components of the weighted Reynolds shear stress and the weighted turbulent heat flux. Meanwhile, the traveling wave-like control input modifies the ratio of the mean velocity and temperature gradients. This causes dissimilarity between the random components of the weighted Reynolds shear stress and the weighted turbulent heat flux away from the wall, although the turbulent Prandtl number remains almost unchanged. The present results show that both the direct and indirect effects contribute to dissimilar heat transfer enhancement to a similar degree.

ACKNOWLEDGEMENTS

The authors acknowledge the financial support by the Ministry of Education, Culture, Sports, Science and Technology of Japan (MEXT) through the Grand-in-Aid for Scientific Research (A) (No. 20246036) and JSPS Postdoctal Fellowship for Research Abroad (YH).

REFERENCES

Fukagata, K., Iwamoto, K. & Kasagi, N., 2002, "Contribution of Reynolds stress distribution to the skin friction in wall-bounded flows," Physics of Fluids, Vol. 14, pp. L73-L76.

Hasegawa, Y. and Kasagi, N., 2010, "Dissimilar Control of Momentum and Heat Transfer in Wall Turbulence," Euromech Fluid Mechanics Conference 8, Bad Reichenhall, Sept. 13-16, S4-30.

Hasegawa, Y. and Kasagi, N., 2011, "Dissimilar Control of Momentum and Heat Transfer in a Fully Developed Turbulent Channel Flow," Journal of Fluid Mechanics, accepted.

Kasagi, N., Hasegawa, Y., Fukagata, K. and Iwamoto, K., 2011, "Control of Turbulent Transport: Less Friction and More Heat Transfer," ASME Journal of Heat Transfer, in press.

Lee, C., Kim, J. and Choi, H., 1998, "Suboptimal control of turbulent channel flow for drag reduction," Journal of Fluid Mechanics, Vol. 358, pp. 245-258.